ANALYSIS OF STRESS INTENSITY FACTORS FOR A PAIR OF EDGE CRACKS IN SEMI-INFINITE MEDIUM WITH DISTRIBUTED EIGENSTRAIN

A.M. AFSAR* and S.R. AHMED
Mechanical Engineering Department
Bangladesh University of Engineering and Technology (BUET)
Dhaka 1000, BANGLADESH
e-mail: mdafsarali@me.buet.ac.bd

This study analyzes stress intensity factors for a pair of edge cracks in a semi-infinite medium with a distribution of eigenstrain and subjected to a far field uniform applied load. The eigenstrain is considered to be distributed arbitrarily over a region of finite depth extending from the free surface. The cracks are represented by a distribution of edge dislocations. By using the complex potential functions of the edge dislocations, a simple effective method is developed to calculate the stress intensity factor for the edge cracks. The method is employed to obtain some numerical results of the stress intensity factor for different distributions of eigenstrain. The numerical results reveal that the stress intensity factor of the edge cracks is significantly influenced by the magnitude as well as distribution of eigenstrain within the finite depth. The eigenstrains that induce compressive stresses at and near the free surface of the semi-infinite medium reduce the stress intensity factor that, in turn, enhances the apparent fracture toughness of the material.

Key words: stress intensity factor, eigenstrain, edge dislocation, edge crack, semi-infinite medium.

1. Introduction

Eigenstrain (Mura, 1987) is the generic name of such non-elastic strains as thermal expansion, phase transformation, initial strains, plastic strains, and mismatch strains. The incompatibility of these eigenstrains results in eigenstresses that are self-equilibrated internal stresses. The free surface of a semi-infinite medium may undergo various kinds of machining processes like cutting, grinding, milling, etc., as well as heat treatment processes. Consequently, eigenstrain is developed at and near the free surface of the medium. Again, the free surface may be exposed to different temperatures than that in other parts of the medium, which results in a nonuniform temperature distribution near the free surface. This also causes the eigenstrain to develop at and near the free surface. The effect of this eigenstrain on the stress intensity factor needs to be analyzed in order to understand and improve the fracture characteristics of the medium. So far, stress intensity factors of edge cracks in semi-infinite media have been studied extensively for various loading conditions, such as, far field uniform load, uniform pressure over part of the crack surface, point load, etc. The works of Stallybrass (1970), Hartranft and Sih (1973), Sneddon and Das (1971), Sneddon (1946), and Afsar (1997) may be cited as a few examples. More recently, Sekine and Afsar (1999) considered a single edge crack in a semi-infinite functionally graded material (FGM) and investigated the effect of eigenstrain on the stress intensity factor followed by the optimization of composition profile for the desired brittle fracture characteristics in the FGM medium. As an extension of their work, they (Afsar and Sekine, 2000) carried out further research to investigate the effect of periodic edge cracks on the material distribution for prescribed fracture characteristics in the semi-infinite medium.

In this study, we concentrate on the two edge cracks in a semi-infinite medium of a homogeneous material with a distributed eigenstrain. It is recognized that an eigenstrain is inherently developed in an FGM body due to a nonuniform coefficient of thermal expansion, as a result of cooling from sintering temperature.

* To whom correspondence should be addressed

However, it may also be developed in a semi-infinite medium of a homogeneous material due to various machining and heat treatment processes. This eigenstrain is considered here for investigating its effects on the stress intensity factor for a pair of edge cracks in the semi-infinite medium of a homogeneous material. In our present analysis, the eigenstrain is assumed to be spread over a region of finite depth only that extends from the free surface. This assumption is fairly reasonable as the various machining and heat treatment processes affect the region whose depth from the free surface is indeed small. For such a problem, a simple and effective method is developed to evaluate the stress intensity factors by using the method of complex potential functions of edge dislocations representing the cracks. To demonstrate the method, some numerical results are obtained and presented for different functional forms of eigenstrain distribution.

2. Model of the problem

A semi-infinite medium shown in Fig.1, is subjected to a far-field uniform applied stress σ_x^0. The region of finite depth w has also an arbitrary distribution of eigenstrain ε^*, which is a function of y only. Shown in the figure are also two edge cracks of equal length *A* and *B*, both of which are perpendicular to the free surface. The length of the cracks and the distance between them are denoted by *a* and *d*, respectively. A principal coordinate system $x-y$ and a secondary coordinate system x_1-y_1 are considered, the origins of which are located at the mouths of cracks *A* and *B*, respectively. If we define two complex variables $z=x+iy$ and $z_1=x_1+iy_1$ that represent the coordinate of a point with reference to the principal and secondary coordinate systems, respectively, the following relationship holds between them

$$z_1 = z - d\,. \tag{2.1}$$

For the model outlined above, a method is developed to evaluate the stress intensity factor for plane stress in order to investigate the effect of eigenstrain on the stress intensity factors.

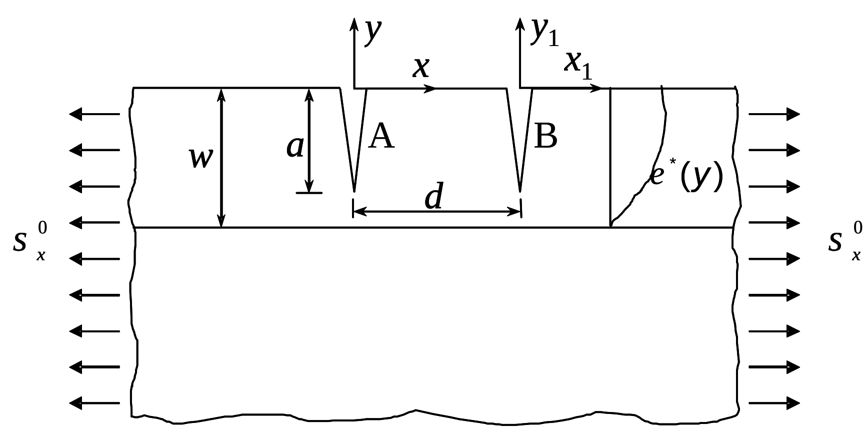

Fig.1. Analytical model of the problem.

3. Stress intensity factor

3.1. Stress field in an uncracked medium

First, we consider the semi-infinite medium without any cracks. The uncracked semi-infinite medium is subjected to a uniform load σ_x^0 along with an arbitrary distribution of the eigenstrain $\varepsilon^*(y)$ in the region of finite depth w. The resultant stress field in the uncracked semi-infinite medium may be determined by superposition of the stress due to the eigenstrain $\varepsilon^*(y)$ and the applied load σ_x^0.

The stress due to eigenstrain $\varepsilon^*(y)$ can be determined following the philosophy outlined by Sekine and Afsar (1999). Since the depth w is very small compared to that of the lower region of the semi-infinite medium, the eigenstrain $\varepsilon^*(y)$ in the region of finite depth w is completely suppressed by the restraining effect from the lower region of the semi-infinite medium. Therefore, the stress developed in the region of finite depth w due to the eigenstrain can be given by

$$\sigma_x^* = -E\varepsilon^* \tag{3.1}$$

where E is the Young's modulus. The stress in the remaining part of the semi-infinite medium due to the eigenstrain is negligible as the region beyond the finite depth w is of infinite dimension over which the stress is distributed. Thus, the resultant stress field in the region of finite depth w is $\left(\sigma_x^* + \sigma_x^0\right)$ while the stress beyond w is equal to the applied stress σ_x^0.

3.2. Cracked semi-infinite medium

The resultant stress field calculated for the uncracked semi-infinite medium in the foregoing is disturbed due to the presence of the cracks A and B. Therefore, it is necessary to determine the redistribution of the stress field in the presence of the cracks. The redistribution of the stress field due to the presence of the cracks is computed by representing the cracks by a continuous distribution of edge dislocations. First, we consider the crack A. As shown in Fig.2, the crack A is represented by a continuous distribution of edge dislocations of densities $b_x^A(s)$ and $b_y^A(s)$, which are the x and y components of the resultant density, respectively. The complex potential functions for these continuous distributions of edge dislocations can be written as (Sekine and Afsar, 1999)

$$\begin{aligned}\Phi^A(z) = &-\frac{i\mu}{\pi(\kappa+1)}\int_0^a\left[\frac{1}{z+is} - \frac{1}{z-is} - \frac{2is}{(z-is)^2}\right] b_x^A(s)ds + \\ &+\frac{\mu}{\pi(\kappa+1)}\int_0^a\left[\frac{1}{z+is} - \frac{1}{z-is} + \frac{2is}{(z-is)^2}\right] b_y^A(s)ds,\end{aligned} \tag{3.2a}$$

$$\begin{aligned}\Psi^A(z) = &\frac{i\mu}{\pi(\kappa+1)}\int_0^a\left[\frac{1}{z+is} - \frac{1}{z-is} - \frac{is}{(z+is)^2} + \frac{3is}{(z-is)^2} - \frac{4s^2}{(z-is)^3}\right] b_x^A(s)ds + \\ &+\frac{\mu}{\pi(\kappa+1)}\int_0^a\left[\frac{1}{z+is} - \frac{1}{z-is} + \frac{is}{(z+is)^2} + \frac{is}{(z-is)^2} - \frac{4s^2}{(z-is)^3}\right] b_y^A(s)ds\end{aligned} \tag{3.2b}$$

where

$\mu =$ shear modulus of rigidity, $\kappa =$ Kolosov's constant,

$\kappa = 3-4\nu$ for plane strain, $\kappa = (3-\nu)/(1+\nu)$ for plane stress.

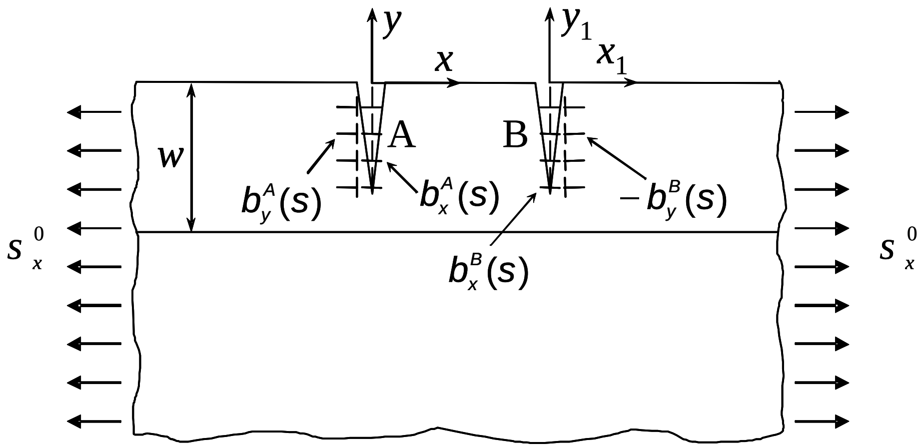

Fig.2. Representation of cracks by continuous distribution of edge dislocations $(0 \geq s \geq -a)$.

The stresses inside an isotropic elastic medium can be expressed in terms of the complex potential functions $\Phi^A(z)$ and $\Psi^A(z)$ and their complex conjugates as follows (Muskhelishvili, 1975)

$$\sigma_{xx}^A + \sigma_{yy}^A = 2\left[\Phi^A(z) + \overline{\Phi^A(z)}\right], \tag{3.3a}$$

$$\sigma_{xx}^A - \sigma_{yy}^A + 2i\sigma_{xy}^A = -2\left[z\overline{\Phi'^A(z)} + \overline{\Psi^A(z)}\right] \tag{3.3b}$$

where the prime represents differentiation with respect to z and the over bar represents the complex conjugate.

Similarly, the stresses for the dislocations representing the crack B as shown in Fig.2 can be given by

$$\sigma_{xx}^B + \sigma_{yy}^B = 2\left[\Phi^B(z_1) + \overline{\Phi^B(z_1)}\right], \tag{3.4a}$$

$$\sigma_{xx}^B - \sigma_{yy}^B + 2i\sigma_{xy}^B = -2\left[z_1\overline{\Phi'^B(z_1)} + \overline{\Psi^B(z_1)}\right] \tag{3.4b}$$

where $\Phi^B(z_1)$ and $\Psi^B(z_1)$ are the complex potential functions for edge dislocations representing the crack B. These functions have the same expressions as those of Eqs (3.2a, b), except that z is replaced by z_1 and the superscript A is replaced by B. Finally, the resultant stresses due to the edge dislocations representing the cracks A and B are obtained by superposition as

$$\sigma_{xx} = \sigma_{xx}^A + \sigma_{xx}^B, \tag{3.5a}$$

$$\sigma_{yy} = \sigma_{yy}^A + \sigma_{yy}^B, \tag{3.5b}$$

$$\sigma_{xy} = \sigma_{xy}^A + \sigma_{xy}^B. \tag{3.5c}$$

Now, the redistributed stress field in the cracked medium can be determined by adding the stress components in Eqs (3.5a-c) to the stress computed for the uncracked semi-infinite medium. The redistributed stress field must satisfy the boundary conditions along the traction free crack surfaces, *i.e.*,

$$\sigma_{xx}^{A}+\sigma_{xx}^{B}+\sigma_{x}^{0}+\sigma_{x}^{*}=0; \qquad x=0, \qquad 0\le y\le -a, \tag{3.6a}$$

$$\sigma_{xy}^{A}+\sigma_{xy}^{B}=0; \qquad x=0, \qquad 0\le y\le -a. \tag{3.6b}$$

It is also noted that the following relationships hold between the dislocation density functions

$$b_x=b_x^A=b_x^B, \tag{3.7a}$$

$$b_y=b_y^A=-b_y^B. \tag{3.7b}$$

Now applying the boundary conditions given by Eqs (3.6a, b) and using the relations in Eqs (2.1) and (3.7a, b), we obtain

$$\frac{2\mu}{\pi(\kappa+1)}\left[\int_0^a\frac{b_x(s)}{y-s}ds+\int_0^a\hat{k}(y,s)b_x(s)ds+\int_0^a\hat{k}_1(y,s)b_x(s)ds-\int_0^a\hat{k}_2(y,s)b_y(s)ds\right]=-\left(\sigma_x^{*}+\sigma_x^{0}\right); \tag{3.8a}$$

$$0\le y\le a,$$

$$\frac{2\mu}{\pi(\kappa+1)}\left[\int_0^a\frac{b_y(s)}{y-s}+\int_0^a\hat{k}(y,s)b_y(s)ds+\int_0^a\hat{k}_3(y,s)b_x(s)ds-\int_0^a\hat{k}_4(y,s)b_y(s)ds\right]=0; \tag{3.8b}$$

$$0\le y\le a$$

where

$$\hat{k}(y,s)=-\frac{1}{y+s}-\frac{2s}{(y+s)^2}+\frac{4s^2}{(y+s)^3}, \tag{3.9a}$$

$$\begin{aligned}\hat{k}_1(y,s)=&\frac{3}{2}\frac{y-s}{(y-s)^2+d^2}-\frac{3}{2}\frac{y+s}{(y+s)^2+d^2}+\\&+\frac{1}{2}\frac{(y+s)^3-3d^2(y+s)}{\left[(y+s)^2+d^2\right]^2}+\frac{1}{2}\frac{3d^2(y-s)-(y-s)^3}{\left[(y-s)^2+d^2\right]^2}+\\&-\frac{2s\left[(y+s)^3(y-s)-6d^2y(y+s)+d^4\right]}{\left[(y+s)^2+d^2\right]^3},\end{aligned} \tag{3.9b}$$

$$\hat{k}_2(y,s)=-\frac{1}{2}\frac{d}{(y-s)^2+d^2}+\frac{1}{2}\frac{d}{(y+s)^2+d^2}+$$
$$+\frac{1}{2}\frac{d(y+s)(5s-3y)+d^3}{\left[(y+s)^2+d^2\right]^2}-\frac{1}{2}\frac{d^3-3d(y-s)^2}{\left[(y-s)^2+d^2\right]^2}+ \tag{3.9c}$$
$$+\frac{2s\left[d^3(y-s)-3d(y+s)^2(y-s)+3d^3(y+s)-d(y+s)^3\right]}{\left[(y+s)^2+d^2\right]^3},$$

$$\hat{k}_3(y,s)=-\frac{1}{2}\frac{d}{(y-s)^2+d^2}+\frac{1}{2}\frac{d}{(y+s)^2+d^2}+$$
$$+\frac{1}{2}\frac{d(y+s)(5s-3y)+d^3}{\left[(y+s)^2+d^2\right]^2}-\frac{1}{2}\frac{d^3-3d(y-s)^2}{\left[(y-s)^2+d^2\right]^2}+ \tag{3.9d}$$
$$-\frac{2s\left[d^3(y-s)-3d(y+s)^2(y-s)+3d^3(y+s)-d(y+s)^3\right]}{\left[(y+s)^2+d^2\right]^3},$$

$$\hat{k}_4(y,\,s)=\frac{1}{2}\frac{y-s}{(y-s)^2+d^2}-\frac{1}{2}\frac{y+s}{(y+s)^2+d^2}+$$
$$-\frac{1}{2}\frac{(y+s)^3-3d^2(y+s)}{\left[(y+s)^2+d^2\right]^2}+\frac{1}{2}\frac{(y-s)^3-3d^2(y-s)}{\left[(y-s)^2+d^2\right]^2}+ \tag{3.9e}$$
$$-\frac{2s\left[(y+s)^3(y-s)-6yd^2(y+s)+d^4\right]}{\left[(y+s)^2+d^2\right]^3}.$$

Equations (3.8a) and (3.8b) are two singular integral equations and it is seen that there is a coupling between the Burgers vectors b_x and b_y which give the Mode I and Mode II stress intensity factors, respectively.

4. Numerical method of solution

An analytical solution to the singular integral equations as given by Eqs (3.8a, b) is not possible. Therefore, a numerical method is adopted to solve the equation. First, the singular integral equation is normalized over the interval $[-1,+1]$ by using the substitutions

$$t=\frac{2s}{a}-1, \tag{4.1a}$$

$$\xi=\frac{2y}{a}-1, \tag{4.1b}$$

$$P=\frac{D}{(a/w)}, \qquad D=\frac{2d}{w}, \tag{4.1c}$$

as

$$\frac{2\mu}{\pi(\kappa+1)}\left[\int_{-1}^{1}\frac{B_x(t)}{(\xi-t)}dt+\int_{-1}^{1}k(\xi,t)B_x(t)dt+\int_{-1}^{1}k_1(\xi,t)B_x(t)dt+\int_{-1}^{1}k_2(\xi,t)B_y(t)dt\right]=$$
$$=-\left[\sigma_x^*(\xi)+\sigma_x^0(\xi)\right];$$
$$-1\le\xi\le 1, \tag{4.2a}$$

$$\frac{2\mu}{\pi(\kappa+1)}\left[\int_{-1}^{1}\frac{B_y(t)}{(\xi-t)}dt+\int_{-1}^{1}k(\xi,t)B_y(t)dt+\int_{-1}^{1}k_3(\xi,t)B_x(t)dt+\int_{-1}^{1}k_4(\xi,t)B_y(t)dt\right]=0;$$
$$-1\le\xi\le 1 \tag{4.2b}$$

where

$$k(\xi,t)=-\frac{1}{t+\xi+2}-\frac{2(t+1)}{(t+\xi+2)^2}+\frac{4(t+1)^2}{(t+\xi+2)^3}, \tag{4.3a}$$

$$k_1(\xi,t)=\frac{3}{2}\frac{(\xi-t)}{\left[(\xi-t)^2+P^2\right]}-\frac{3}{2}\frac{(\xi+t+2)}{\left[(\xi+t+2)^2+P^2\right]}+$$
$$+\frac{1}{2}\frac{(\xi+t+2)^3-3P^2(\xi+t+2)}{\left[(\xi+t+2)^2+P^2\right]^2}+\frac{1}{2}\frac{3P^2(\xi-t)-(\xi-t)^3}{\left[(\xi-t)^2+P^2\right]^2}+$$
$$-\frac{2(t+1)\left[(\xi+t+2)^3(\xi-t)-6P^2(\xi+1)(\xi+t+2)+P^4\right]}{\left[(\xi+t+2)^2+P^2\right]^3}, \tag{4.3b}$$

$$k_2(\xi,t)=-\frac{1}{2}\frac{P}{\left[(\xi-t)^2+P^2\right]}+\frac{1}{2}\frac{P}{\left[(\xi+t+2)^2+P^2\right]}+$$
$$+\frac{1}{2}\frac{P(\xi+t+2)(5t-3\xi+2)+P^3}{\left[(\xi+t+2)^2+P^2\right]^2}-\frac{1}{2}\frac{P^3-3P(\xi-t)^2}{\left[(\xi-t)^2+P^2\right]^2}+$$
$$+2(t+1)\left[P^3(\xi-t)-3P(\xi+t+2)^2(\xi-t)+\right.$$
$$\left.+3P^3(\xi+t+2)-P(\xi+t+2)^3\right]\Big/\left[(\xi+t+2)^2+P^2\right]^3, \tag{4.3c}$$

$$k_3(\xi,t) = -\frac{1}{2}\frac{P}{\left[(\xi-t)^2+P^2\right]} + \frac{1}{2}\frac{P}{\left[(\xi+t+2)^2+P^2\right]} +$$
$$+\frac{1}{2}\frac{P(\xi+t+2)(5t-3\xi+2)+P^3}{\left[(\xi+t+2)^2+P^2\right]^2} - \frac{1}{2}\frac{P^3-3P(\xi-t)^2}{\left[(\xi-t)^2+P^2\right]^2} + \tag{4.3d}$$
$$-2(t+1)\Big[P^3(\xi-t) - 3P(\xi+t+2)^2(\xi-t) +$$
$$+3P^3(\xi+t+2) - P(\xi+t+2)^3\Big] \Big/ \left[(\xi+t+2)^2+P^2\right]^3,$$

$$k_4(\xi,t) = \frac{1}{2}\frac{(\xi-t)}{\left[(\xi-t)^2+P^2\right]} - \frac{1}{2}\frac{(\xi+t+2)}{\left[(\xi+t+2)^2+P^2\right]} +$$
$$-\frac{1}{2}\frac{(\xi+t+2)^3-3P^2(\xi+t+2)}{\left[(\xi+t+2)^2+P^2\right]^2} - \frac{1}{2}\frac{3P^2(\xi-t)-(\xi-t)^3}{\left[(\xi-t)^2+P^2\right]^2} + \tag{4.3e}$$
$$-\frac{2(t+1)\left[(\xi+t+2)^3(\xi-t)-6P^2(\xi+1)(\xi+t+2)+P^4\right]}{\left[(\xi+t+2)^2+P^2\right]^3},$$

$$B_x(t) = b_x(s), \qquad B_y(s) = b_y(y). \tag{4.3f}$$

The dislocation density functions $B_x(t)$ and $B_y(t)$ can be expressed as the product of a fundamental function $W(t)$, which characterizes the bounded-singular behavior of $B_x(t)$ and $B_y(t)$, and a bounded continuous function $\varphi_x(t)$ and $\varphi_y(t)$ in the closed interval $[-1,+1]$. Thus

$$B_x(t) = W(t)\varphi_x(t), \tag{4.4a}$$

$$B_y(t) = W(t)\varphi_y(t). \tag{4.4b}$$

Using the Gauss-Jacobi integral formula in the manner similar to that developed by Erdogan *et al*. (1973), the singular integral equation can be converted to a system of linear algebraic equations to determine the unknowns $\varphi_x(t)$ and $\varphi_y(t)$ as

$$\frac{2\mu}{(\kappa+1)}\left[\sum_{k=1}^{n}\varphi_x(t_k)(1+t_k)\left\{\frac{1}{\xi_r-t_k}+k(\xi_r,t_k)+k_1(\xi_r,t_k)\right\}+\sum_{k=1}^{n}\varphi_y(t_k)(1+t_k)k_2(\xi_r,t_k)\right]=$$
$$=-\frac{2n+1}{2}\left[\sigma_x^*(\xi_r)+\sigma_x^0(\xi_r)\right], \tag{4.5a}$$
$$r = 1,2,3,\ \ldots..,\ n,$$

$$\frac{2\mu}{(\kappa+1)}\left[\sum_{k=1}^{n}\varphi_x(t_k)(1+t_k)k_3(\xi_r,\,t_k)+\right.$$
$$\left.+\sum_{k=1}^{n}\varphi_y(t_k)(1+t_k)\left\{\frac{1}{\xi_r-t_k}+k(\xi_r,\,t_k)+k_4(\xi_r,\,t_k)\right\}\right]=0;$$
$$r=1,2,3,\ldots..,n \tag{4.5b}$$

where the integration and collocation points are, respectively, given by (Hills *et al.*, 1996)

$$t_k=\cos\left(\frac{2k-1}{2n+1}\pi\right),\qquad k=1,2,3,\ldots...,n, \tag{4.6a}$$

$$\xi_r=\cos\left(\frac{2r\pi}{2n+1}\right),\qquad r=1,2,3,\ldots...,n. \tag{4.6b}$$

It can readily be shown that the Mode I and II stress intensity factors can be derived as (Hills *et al.*, 1996)

$$K_{\mathrm{I,II}}=\sqrt{\pi a}\,\frac{2\mu}{(\kappa+1)}\sqrt{2}\varphi_{x,y}(+1). \tag{4.7}$$

The solution of Eqs (4.5a, b) provides the values of φ_x and φ_y only at the integration points t_k. The calculation of stress intensity factors, as seen from Eq.(4.7), requires the values of these functions at the crack tip, i.e., $\varphi_x(+1)$ and $\varphi_y(+1)$. These values can be obtained by the following Krenk's (1975) interpolation formula

$$\varphi_{x,y}(+1)=\frac{2}{2n+1}\sum_{i=1}^{n}\frac{\sin\left(\frac{2i-1}{2n+1}n\pi\right)}{\tan\left(\frac{2i-1}{2n+1}\frac{\pi}{2}\right)}\varphi_{x,y}(t_i). \tag{4.8}$$

Using Eqs. (4.5a, b) through (4.8), stress intensity factors can be calculated for a given applied load and eigenstrain distribution.

5. Numerical results and discussion

In this section, some numerical results of stress intensity factors are calculated and presented for various distributions of the eigenstrain in the region of finite depth w of the semi-infinite medium. The distributions of the eigenstrain considered are parabolic 1 distribution: $\varepsilon_{xx}^{*}=\varepsilon^{0}\left(1+\frac{y}{w}\right)^{\frac{1}{2}}$, parabolic 2 distribution: $\varepsilon_{xx}^{*}=\varepsilon^{0}\left(1-\frac{y^2}{w^2}\right)$, parabolic 3 distribution: $\varepsilon_{xx}^{*}=\varepsilon^{0}\left(1+\frac{y}{w}\right)^{2}$, linear distribution:

$\varepsilon^{*}_{xx}=\varepsilon\left(1+\dfrac{y}{w}\right)$, and uniform distribution: $\varepsilon^{*}_{xx}=\varepsilon^{0}$. These distributions of the eigenstrain are shown in Fig.3. The above five distributions have been chosen merely as examples. In the numerical calculation, the number of collocation and integration points n is taken as *100*, for which the values of the stress intensity factors, calculated by setting $\varepsilon^{0}=0$, agree well with those obtained by Ishida (1979) as shown in Tab.1. When $\varepsilon^{0}=0$, the problem reduces to the semi-infinite medium subjected to the applied load only.

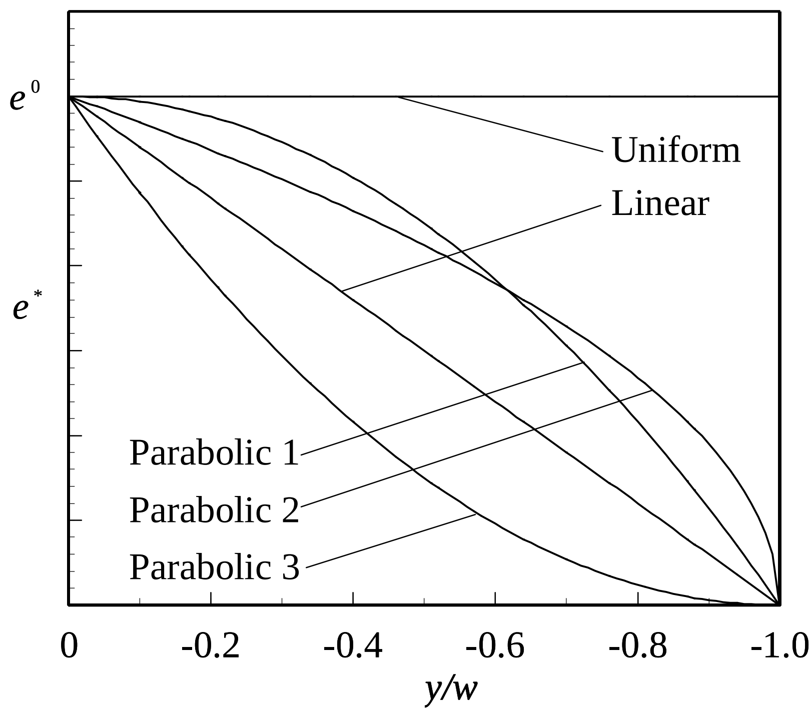

Fig.3. Distribution of eigenstrains in the region of finite depth *w*.

Table 1. Comparison of stress intensity factors predicted by the present model with those predicted by Isida (1979) for two edge cracks in a semi-infinite medium under uniform tension.

d/a	K_{I}		K_{II}	
	Present model	M. Isida	Present model	M. Isida
0.1	*0.776905*	*0.777*	*0.1994*	*0.2*
0.2	*0.788869*	*0.789*	*0.1853*	*0.18*
0.5	*0.817194*	*0.817*	*0.1594*	*0.16*
1.0	*0.854256*	*0.854*	*0.1331*	*0.13*
2.0	*0.911070*	*0.911*	*0.0909*	*0.09*
3.0	*0.964360*	*0.964*	*0.0541*	*0.053*
4.0	*1.007198*	*1.007*	*0.0316*	*0.030*
6.0	*1.058003*	*1.058*	*0.0123*	*0.012*
8.0	*1.082487*	*1.082*	*0.0058*	*0.006*

Figure 4a exhibits the Mode I and Mode II stress intensity factors as a function of normalized crack length a/w and normalized crack spacing d/w. The stress intensity factors are also normalized dividing them by the true value of the stress intensity factor $K_e = 1.12152$ for a single edge crack in a semi-infinite medium under a far field uniform load σ_x^0 only. The results correspond to the parabolic 1 distribution of the eigenstrain as shown in Fig.3. In calculating the stress intensity factor, we define a parameter $\gamma = E\varepsilon^0 / \sigma_x^0$ in which ε^0 is the eigenstrain at $y = 0$ and E is the Young's modulus of the material. The parameter γ, in fact, is the ratio of eigenstress at $y = 0$ to the applied stress σ_x^0. The stress intensity factors shown in Fig.4a are obtained for $\gamma = 0.5$. The broken lines represent the Mode II stress intensity factors while the solid lines represent the Mode I stress intensity factors. It is noted that the Mode II stress intensity factors are only a small fraction of the Mode I stress intensity factors. For a small value of the crack spacing, the Mode II stress intensity factor is higher and it decreases as the crack spacing increases implying that the effect of one crack on the other diminishes. The Mode I stress intensity factor has the reverse trend of the Mode II stress intensity factor. The Mode I stress intensity factor increases with the increase of the crack spacing d/w. The eigenstrain is distributed over the region of finite depth w and the crack tip crosses the region of the eigenstrain when $a/w \geq 1$ showing points of inflection on the curves of the stress intensity factor. Figures 4b through 4e depict the normalized stress intensity factors for parabolic 2, parabolic 3, linear, and uniform distributions of the eigenstrain, respectively. The curves of all the figures have the same characteristics except that the Mode I stress intensity factors for the uniform distribution of the eigenstrain have quite sharp points of inflection at $a/w = 1$.

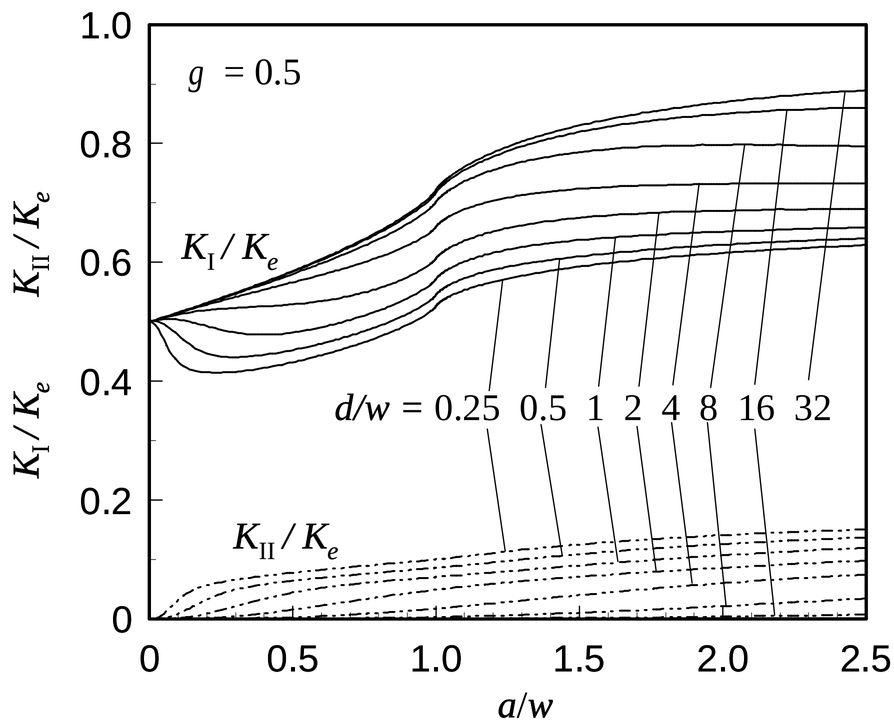

Fig.4(a). Normalized stress intensity factors for parabolic 1 distribution of eigenstrain $(\gamma = 0.5)$.

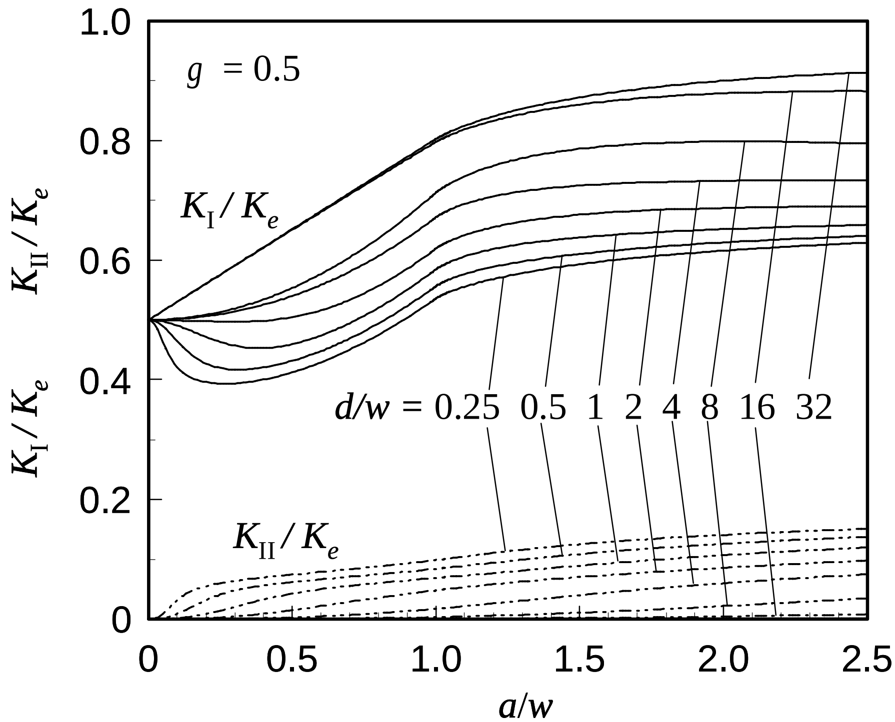

Fig.4(b). Normalized stress intensity factors for parabolic 2 distribution of eigenstrain $(\gamma = 0.5)$.

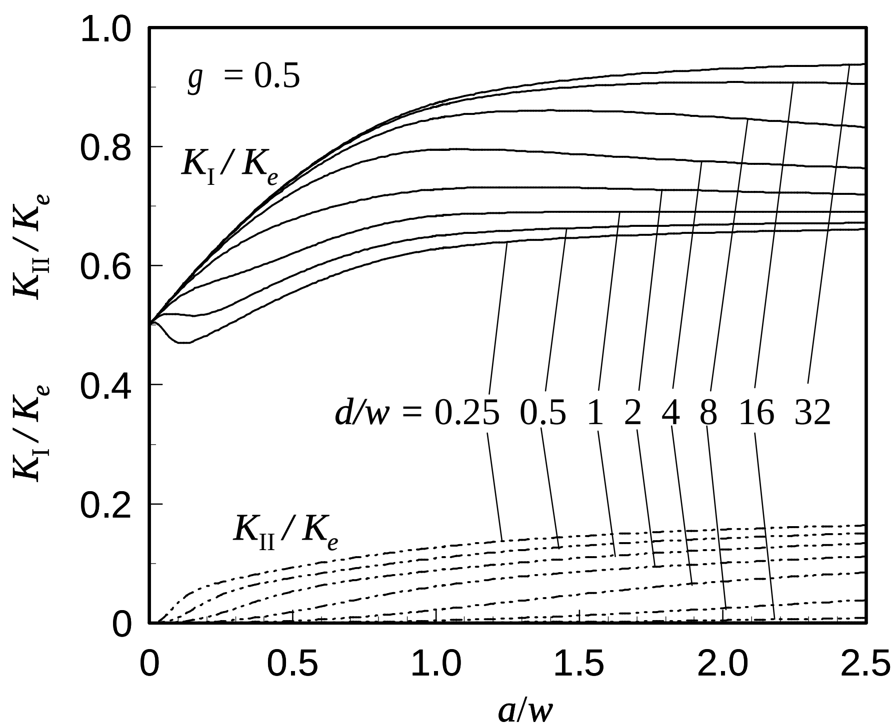

Fig.4(c). Normalized stress intensity factors for parabolic 3 distribution of eigenstrain $(\gamma = 0.5)$.

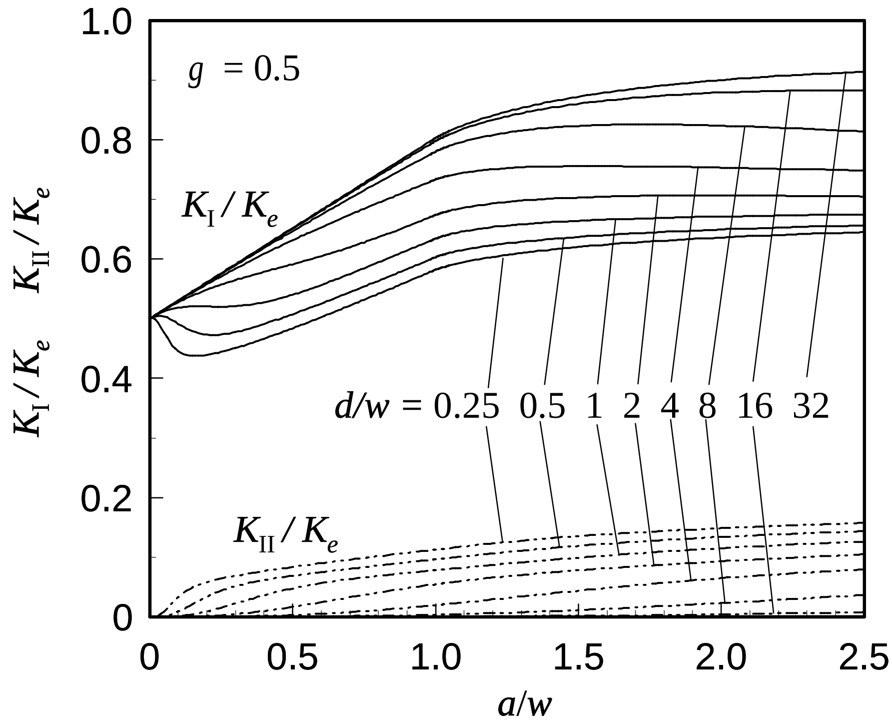

Fig.4(d). Normalized stress intensity factors for linear distribution of eigenstrain $(\gamma = 0.5)$.

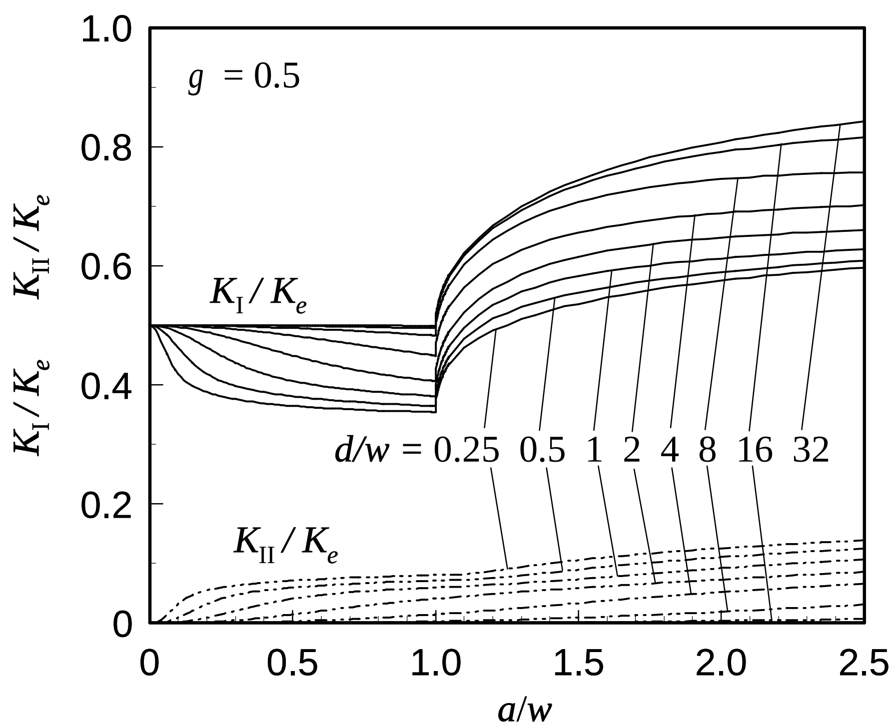

Fig.4(e). Normalized stress intensity factors for uniform distribution of eigenstrain $(\gamma = 0.5)$.

Figure 5 illustrates the effect of the type of the eigenstrain distribution on the stress intensity factors. Both the Mode II and Mode I stress intensity factors are plotted for the five different distributions of the eigenstrain as shown in Fig.3. The uniform distribution of the eigenstrain is associated with the minimum stress intensity factor while the parabolic 3 distribution of the eigenstrain gives the maximum stress intensity factor. The average eigenstrain over the region of finite depth w is the maximum for the uniform distribution of the eigenstrain among all the five distributions. This, in turn, induces the maximum magnitude of average compressive eigenstress that has a reducing effect on the resultant stress intensity factor. Therefore, the uniform distribution of the eigenstrain gives the minimum stress intensity factor. On the other hand, the parabolic 3 distribution of the eigenstrain has the minimum average value of the eigenstrain over the region of finite depth w. This induces an average compressive eigenstress of the lowest magnitude attributing the least in the reduction of the resultant stress intensity factor. The other three curves for each mode of the stress intensity factor in Fig.5 fall between the two curves corresponding to the uniform and parabolic 3 distributions of the eigenstrain. This is due to the fact that the average values of these three distributions of the eigenstrain fall between the average values of the uniform and parabolic 3 distributions of the eigenstrain.

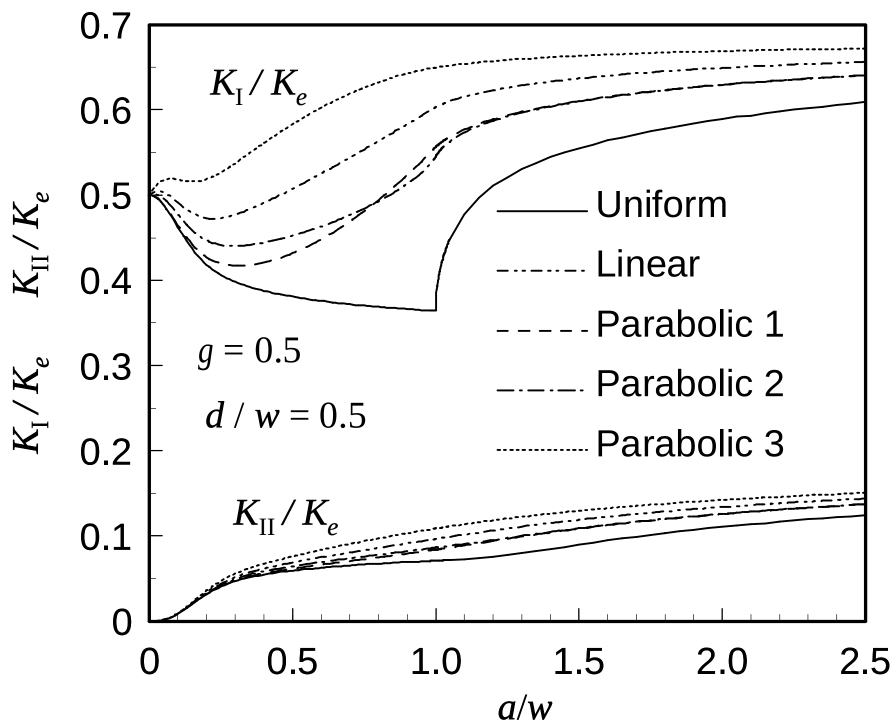

Fig.5. Effects of the distribution of eigenstrain on stress intensity factors.

The normalized Mode I stress intensity factors as a function of the parameter γ and normalized crack length a/w are shown in Fig.6a. The results correspond to $d/w = 0.5$ and the linear distribution of the eigenstrain. The higher value of γ indicates the higher magnitude of the eigenstrain at $y = 0$. This implies that the compressive eigenstress at $y = 0$ has also a higher value. Thus, the stress intensity factor has a lower value when γ is higher. As stated earlier, the compressive eigenstress associated with the eigenstrain reduces the stress intensity factor. If there were no eigenstrain in the semi-infinite medium, the normalized stress intensity factor would be unity for a small value of normalized crack length a/w. Because the small value of a/w implies that the distance d between the cracks is large compared to the crack length a. Thus, one can reasonably obtain the value of stress intensity factor for a single crack in the semi-infinite medium subjected to the applied load σ_x^0 only, which will give the ratio $K_I/K_e = 1$. However, the value of the ratio K_I/K_e is less than unity for a small value of a/w because of the eigenstrain in the finite region of depth *w* of the semi-infinite medium. Considering the case of $\gamma = 0.5$ as an example, it is noted that the magnitude of eigenstress associated with the eigenstrain at $y = 0$ is *50%* of the applied load for which the stress intensity factor K_I is also *50%* of the stress intensity factor K_e, the value of a single crack when the semi-infinite medium is subjected to the applied load σ_x^0 only. There is also another important point to be noted. When γ exceeds unity, crack closure occurs up to certain length of the crack, i.e., the crack surfaces are in contact and no stress, i.e., intensity occurs. As an example, the stress intensity occurs only when a/w exceeds *0.5* for $\gamma = 1.5$.

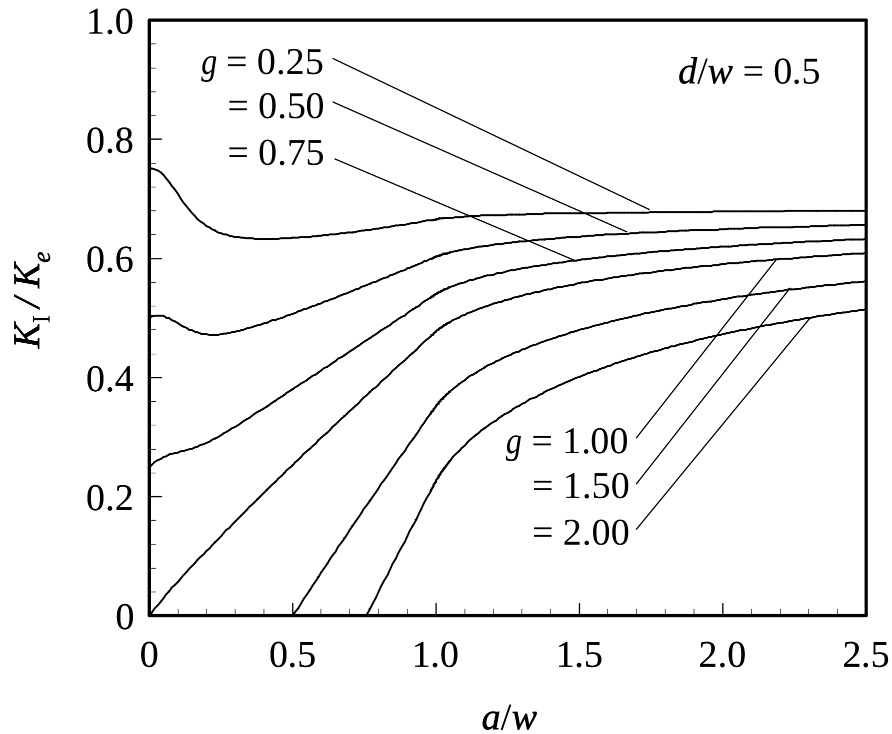

Fig.6(a). Normalized Mode I stress intensity factors as a function of normalized crack length and parameter γ for linear distribution of eigenstrain.

Figure 6b illustrates the normalized Mode II stress intensity factors as a function of parameter γ and normalized crack length a/w for a normalized crack spacing $d/w = 0.5$. The results are plotted for the linear distribution of the eigenstrain. Here, we remember that the Mode II stress intensity occurs though the semi-infinite medium is subjected to mode I loading only. The Mode II stress intensity factors are related to the sliding of the crack surfaces relative to each other in the direction parallel to the crack surfaces. It is noted that these stress intensity factors are also decreased as the parameter γ increases. However, it is noted that the Mode II stress intensity factor is negative up to a certain crack length and positive when the crack length further increases for γ greater than unity. This implies that a crack surface alters its sliding direction with respect to the other during the crack growth.

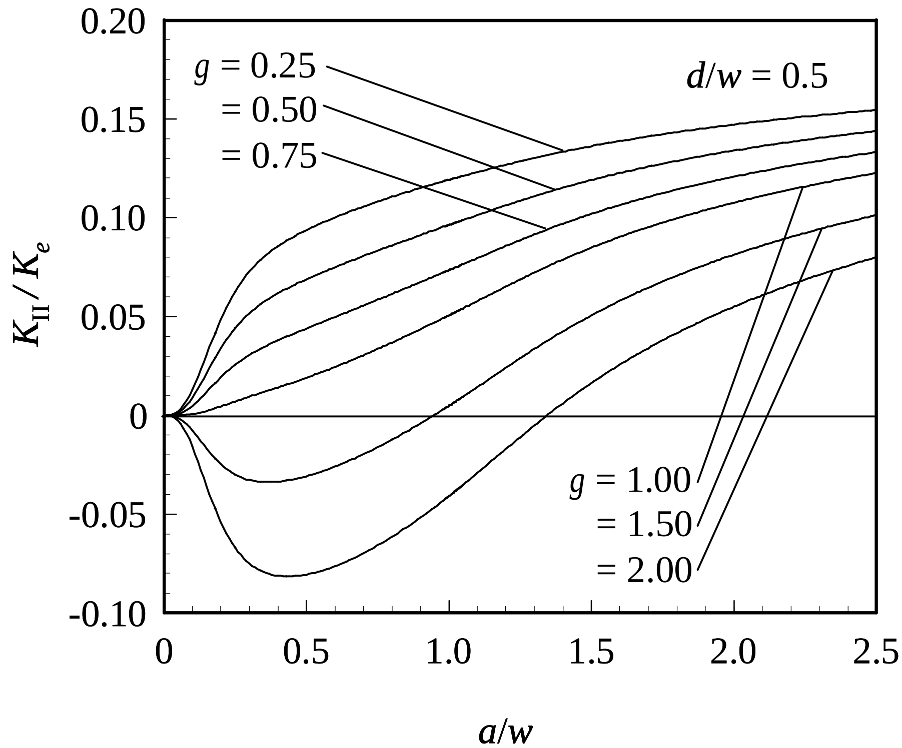

Fig.6(b). Normalized Mode II stress intensity factors as a function of normalized crack length and parameter γ for linear distribution of eigenstrain.

In Fig.7a, normalized Mode I stress intensity factors are plotted as a function of normalized crack spacing d/w keeping the value of normalized crack length a/w constant ($a/w=0.5$). In the lower range of crack spacing, the stress intensity factor enhances as the distance ***d*** increases. After a certain value of ***d***, the stress intensity factor becomes constant that indicates that one crack has no effect on the other, i.e., the single crack phenomenon is attained. Figure 7b displays the corresponding Mode II stress intensity factors as a function of crack spacing d/w for the constant value of $a/w=0.5$. From a small value of γ to unity, the stress intensity factors gradually decrease to zero with the increase of crack spacing d/w. The zero value of the stress intensity factors indicates that the cracks are far away from each other, and a single crack phenomenon is obtained, i.e., the Mode II stress intensity disappears. For values of γ higher than unity, the stress intensity factors increase from a negative value to zero with the increase of the crack spacing d/w indicating the same phenomena as before. However, in this case, the direction of sliding of the crack surfaces is opposite to that for small values of γ, i.e., for $\gamma \le 1$.

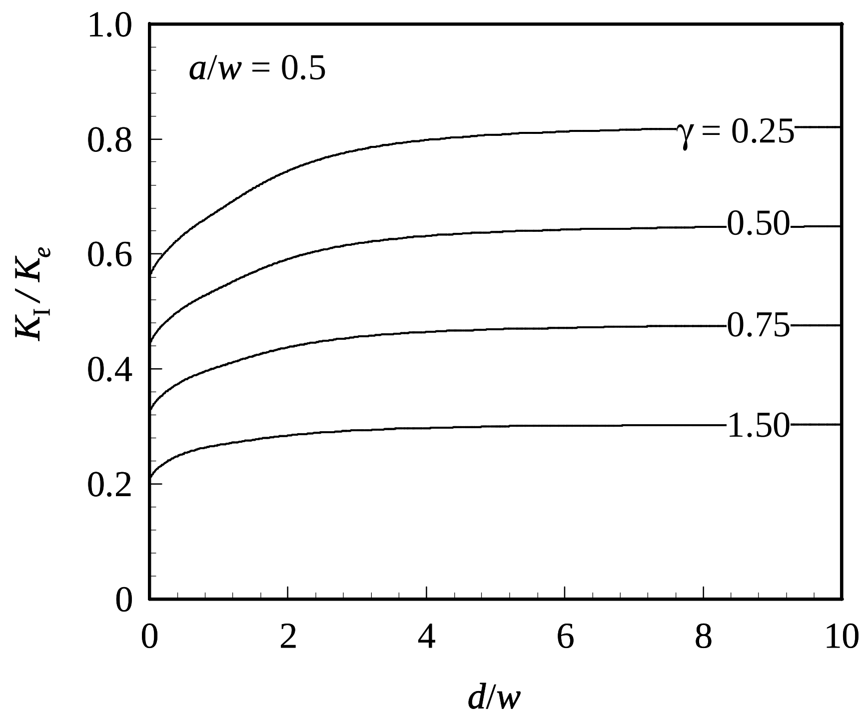

Fig.7(a). Normalized Mode I stress intensity factors as a function of normalized crack spacing and parameter γ for linear distribution of eigenstrain.

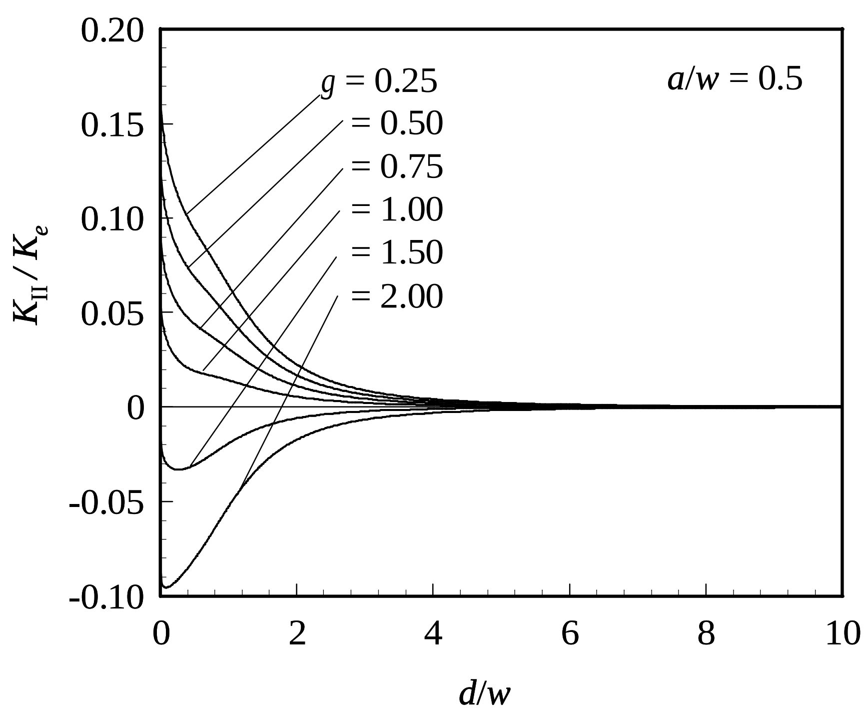

Fig.7(b). Normalized Mode II stress intensity factors as a function of normalized crack spacing and parameter γ for linear distribution of eigenstrain.

6. Conclusions

A simple and effective method is developed to analyze stress intensity factors for a pair of edge cracks in a semi-infinite medium with any arbitrary distribution of the eigenstrain and subjected to a far field applied load. The method can be applied to calculate the stress intensity factors for a single edge crack by using a large value of the distance between the cracks. From the numerical results, it is noted that the stress intensity factors significantly depend on the distribution of the eigenstrain. The positive eigenstrain induces a compressive eigenstress that reduces the stress intensity factors. This reduction of the stress intensity factors is attributed to the toughening of the material. The higher magnitude of an average eigenstrain has a greater effect on the stress intensity factors. With increasing the value of crack spacing, the Mode I stress intensity factors increase while the Mode II stress intensity factors decrease. For higher values of the eigenstrain, as the crack length increases, the Mode II stress intensity factors change sign from negative to positive, thereby indicating that the crack surfaces alter their sliding direction during crack growth.

Nomenclature

a – crack length
$b_x^A, b_x^B, b_y^A, b_y^B, B_x, B_y$ – dislocation density functions
d – distance between the cracks
E – Young's modulus
$K_{\mathrm{I}}, K_{\mathrm{II}}$ – stress intensity factors
s – distance along the crack line
t_k – integration points
w – depth from free surface
$x-y$ – principal coordinate system
$x_1 - y_1$ – secondary coordinate system
z – complex variable $(z = x + iy)$
ε^* – eigenstrain
κ – Kolosov's constant
μ – shear modulus
ν – Poisson's ratio
ξ_r – collocation points
σ_x^0 – applied stress
σ_x^* – eigenstress
Φ, Ψ – complex potential functions

References

Afsar A.M. (1997): *Analysis of Edge Cracks in Semi-Infinite Functionally Gradient Materials with Distributed Eigenstrains*. – M. Sc. Dissertation, Tohoku University, Japan.

Afsar A.M. and Sekine H. (2000): *Crack spacing effect on the brittle fracture characteristics of semi-infinite functionally graded materials with periodic edge cracks*. – International Journal of Fracture, vol.102, No.2, pp.L61-L66.

Erdogan F., Gupta G.D. and Cook T.S. (1973): *Numerical solution of singular integral equations*, In: Methods of Analysis and Solutions of Crack Problems (G.C. Sih, Ed.). – Leyden 1: Noordhoff International Publishing.

Hartranft R.J. and Sih G.C. (1973): *Alternating method applied to edge and surface crack problems,* In: Methods of Analysis and Solutions of Crack Problems 1 (G.C. Sih, Ed.). – Leyden: Noordhoff International Publishing.

Hills D.A., Kelly P.A., Dai D.N. and Korsunsky A.M. (1996): ***Distributed dislocation fundamentals***, In: Solution of Crack Problems-The Distributed Dislocation Technique (G.M.L. Gladwell, Ed.). – Dordrecht/Boston/London: Kluwer Academic Punlishers.

Isida M. (1979): ***Tension of a half plane containing array cracks, branched cracks and cracks emanating from sharp notches.*** – Transaction of the Japan Society of Mechanical Engineers, vol.45, No.392, pp.306-317.

Krenk S. (1975): ***On the use of the interpolation polynomial for solution of singular integral equation.*** – Quarterly of Applied Mathematics, vol.32, No.4, pp.479-484.

Mura T. (1987): ***General theory of eigenstrain,*** In: Micromechanics of Defects in Solids-Mechanics of Elastic and Inelastic solids 3. (S. Nemat-Nasser and G.A.E. Oravas, Ed.). – Dordrecht/Boston/London: Kluwer Academic Publishers.

Muskhelishvili N.I. (1975): ***Some Basic Problems of the Mathematical Theory of Elasticity (Translated from the Russian by J. R. M. Radok)***. – The Netherlands: Noordhoff International Publishers.

Sekine H. and Afsar A.M. (1999): ***Composition profile for improving the brittle fracture characteristics in semi-infinite functionally graded materials.*** – JSME International Journal, Series A, vol.42, No.4, pp.592-600.

Sneddon I.N. (1946): ***The distribution of stress in the neighborhood of a crack in an elastic solid.*** - Proceedings of the Royal Society of London, 187A, pp.229-260.

Sneddon I.N. and Das S.C. (1971): ***The stress intensity factor at the tip of an edge crack in an elastic half-plane.*** – International Journal of Engineering Science, vol.9, pp.25-36.

Stallybrass M.P. (1970): ***A crack perpendicular to an elastic half-plane.*** – International Journal of Engineering Science, vol.8, pp.351-362.

Received: August 3, 2004

Revised: Februay 23, 2005